Searches for isospin-violating transitions $\chi_{c0,2}\to\pi^{0}\eta_{c}$

M. Ablikim *et al.* (BESIII Collaboration)

Phys. Rev. D **91**, 112018 — Published 30 June 2015

DOI: 10.1103/PhysRevD.91.112018

Searches for isospin-violating transitions $\chi_{c0,2} \to \pi^0\eta_c$

M. Ablikim[1], M. N. Achasov[8,a], X. C. Ai[1], O. Albayrak[4], M. Albrecht[3], D. J. Ambrose[43], A. Amoroso[47A,47C], F. F. An[1], Q. An[44], J. Z. Bai[1], R. Baldini Ferroli[19A], Y. Ban[30], D. W. Bennett[18], J. V. Bennett[4], M. Bertani[19A], D. Bettoni[20A], J. M. Bian[42], F. Bianchi[47A,47C], E. Boger[22,h], O. Bondarenko[24], I. Boyko[22], R. A. Briere[4], H. Cai[49], X. Cai[1], O. Cakir[39A,b], A. Calcaterra[19A], G. F. Cao[1], S. A. Cetin[39B], J. F. Chang[1], G. Chelkov[22,c], G. Chen[1], H. S. Chen[1], H. Y. Chen[2], J. C. Chen[1], M. L. Chen[1], S. J. Chen[28], X. Chen[1], X. R. Chen[25], Y. B. Chen[1], H. P. Cheng[16], X. K. Chu[30], G. Cibinetto[20A], D. Cronin-Hennessy[42], H. L. Dai[1], J. P. Dai[33], A. Dbeyssi[13], D. Dedovich[22], Z. Y. Deng[1], A. Denig[21], I. Denysenko[22], M. Destefanis[47A,47C], F. De Mori[47A,47C], Y. Ding[26], C. Dong[29], J. Dong[1], L. Y. Dong[1], M. Y. Dong[1], S. X. Du[51], P. F. Duan[1], J. Z. Fan[38], J. Fang[1], S. S. Fang[1], X. Fang[44], Y. Fang[1], L. Fava[47B,47C], F. Feldbauer[21], G. Felici[19A], C. Q. Feng[44], E. Fioravanti[20A], M. Fritsch[13,21], C. D. Fu[1], Q. Gao[1], Y. Gao[38], Z. Gao[44], I. Garzia[20A], C. Geng[44], K. Goetzen[9], W. X. Gong[1], W. Gradl[21], M. Greco[47A,47C], M. H. Gu[1], Y. T. Gu[11], Y. H. Guan[1], A. Q. Guo[1], L. B. Guo[27], Y. Guo[1], Y. P. Guo[21], Z. Haddadi[24], A. Hafner[21], S. Han[49], Y. L. Han[1], X. Q. Hao[14], F. A. Harris[41], K. L. He[1], Z. Y. He[29], T. Held[3], Y. K. Heng[1], Z. L. Hou[1], C. Hu[27], H. M. Hu[1], J. F. Hu[47A], T. Hu[1], Y. Hu[1], G. M. Huang[5], G. S. Huang[44], H. P. Huang[49], J. S. Huang[14], X. T. Huang[32], Y. Huang[28], T. Hussain[46], Q. Ji[1], Q. P. Ji[29], X. B. Ji[1], X. L. Ji[1], L. L. Jiang[1], L. W. Jiang[49], X. S. Jiang[1], J. B. Jiao[32], Z. Jiao[16], D. P. Jin[1], S. Jin[1], T. Johansson[48], A. Julin[42], N. Kalantar-Nayestanaki[24], X. L. Kang[1], X. S. Kang[29], M. Kavatsyuk[24], B. C. Ke[4], R. Kliemt[13], B. Kloss[21], O. B. Kolcu[39B,d], B. Kopf[3], M. Kornicer[41], W. Kuehn[23], A. Kupsc[48], W. Lai[1], J. S. Lange[23], M. Lara[18], P. Larin[13], C. H. Li[1], Cheng Li[44], D. M. Li[51], F. Li[1], G. Li[1], H. B. Li[1], J. C. Li[1], Jin Li[31], K. Li[12], K. Li[32], P. R. Li[40], T. Li[32], W. D. Li[1], W. G. Li[1], X. L. Li[32], X. M. Li[11], X. N. Li[1], X. Q. Li[29], Z. B. Li[37], H. Liang[44], Y. F. Liang[35], Y. T. Liang[23], G. R. Liao[10], D. X. Lin[13], B. J. Liu[1], C. X. Liu[1], F. H. Liu[34], Fang Liu[1], Feng Liu[5], H. B. Liu[11], H. H. Liu[15], H. H. Liu[1], H. M. Liu[1], J. Liu[1], J. P. Liu[49], J. Y. Liu[1], K. Liu[38], K. Y. Liu[26], L. D. Liu[30], P. L. Liu[1], Q. Liu[40], S. B. Liu[44], X. Liu[25], X. X. Liu[40], Y. B. Liu[29], Z. A. Liu[1], Zhiqiang Liu[1], Zhiqing Liu[21], H. Loehner[24], X. C. Lou[1,e], H. J. Lu[16], J. G. Lu[1], R. Q. Lu[17], Y. Lu[1], Y. P. Lu[1], C. L. Luo[27], M. X. Luo[50], T. Luo[41], X. L. Luo[1], M. Lv[1], X. R. Lyu[40], F. C. Ma[26], H. L. Ma[1], L. L. Ma[32], Q. M. Ma[1], S. Ma[1], T. Ma[1], X. N. Ma[29], X. Y. Ma[1], F. E. Maas[13], M. Maggiora[47A,47C], Q. A. Malik[46], Y. J. Mao[30], Z. P. Mao[1], S. Marcello[47A,47C], J. G. Messchendorp[24], J. Min[1], T. J. Min[1], R. E. Mitchell[18], X. H. Mo[1], Y. J. Mo[5], C. Morales Morales[13], K. Moriya[18], N. Yu. Muchnoi[8,a], H. Muramatsu[42], Y. Nefedov[22], F. Nerling[13], I. B. Nikolaev[8,a], Z. Ning[1], S. Nisar[7], S. L. Niu[1], X. Y. Niu[1], S. L. Olsen[31], Q. Ouyang[1], S. Pacetti[19B], P. Patteri[19A], M. Pelizaeus[3], H. P. Peng[44], K. Peters[9], J. L. Ping[27], R. G. Ping[1], R. Poling[42], Y. N. Pu[17], M. Qi[28], S. Qian[1], C. F. Qiao[40], L. Q. Qin[32], N. Qin[49], X. S. Qin[1], Y. Qin[30], Z. H. Qin[1], J. F. Qiu[1], K. H. Rashid[46], C. F. Redmer[21], H. L. Ren[17], M. Ripka[21], G. Rong[1], X. D. Ruan[11], V. Santoro[20A], A. Sarantsev[22,f], M. Savrié[20B], K. Schoenning[48], S. Schumann[21], W. Shan[30], M. Shao[44], C. P. Shen[2], P. X. Shen[29], X. Y. Shen[1], H. Y. Sheng[1], M. R. Shepherd[18], W. M. Song[1], X. Y. Song[1], S. Sosio[47A,47C], S. Spataro[47A,47C], G. X. Sun[1], J. F. Sun[14], S. S. Sun[1], Y. J. Sun[44], Y. Z. Sun[1], Z. J. Sun[1], Z. T. Sun[18], C. J. Tang[35], X. Tang[1], I. Tapan[39C], E. H. Thorndike[43], M. Tiemens[24], D. Toth[42], M. Ullrich[23], I. Uman[39B], G. S. Varner[41], B. Wang[29], B. L. Wang[40], D. Wang[30], D. Y. Wang[30], K. Wang[1], L. L. Wang[1], L. S. Wang[1], M. Wang[32], P. Wang[1], P. L. Wang[1], Q. J. Wang[1], S. G. Wang[30], W. Wang[1], X. F. Wang[38], Y. D. Wang[19A], Y. F. Wang[1], Y. Q. Wang[21], Z. Wang[1], Z. G. Wang[1], Z. H. Wang[44], Z. Y. Wang[1], T. Weber[21], D. H. Wei[10], J. B. Wei[30], P. Weidenkaff[21], S. P. Wen[1], U. Wiedner[3], M. Wolke[48], L. H. Wu[1], Z. Wu[1], L. G. Xia[38], Y. Xia[17], D. Xiao[1], Z. J. Xiao[27], Y. G. Xie[1], Q. L. Xiu[1], G. F. Xu[1], L. Xu[1], Q. J. Xu[12], Q. N. Xu[40], X. P. Xu[36], L. Yan[44], W. B. Yan[44], W. C. Yan[44], Y. H. Yan[17], H. X. Yang[1], L. Yang[49], Y. Yang[5], Y. X. Yang[10], H. Ye[1], M. Ye[1], M. H. Ye[6], J. H. Yin[1], B. X. Yu[1], C. X. Yu[29], H. W. Yu[30], J. S. Yu[25], C. Z. Yuan[1], W. L. Yuan[28], Y. Yuan[1], A. Yuncu[39B,g], A. A. Zafar[46], A. Zallo[19A], Y. Zeng[17], B. X. Zhang[1], B. Y. Zhang[1], C. Zhang[28], C. C. Zhang[1], D. H. Zhang[1], H. H. Zhang[37], H. Y. Zhang[1], J. J. Zhang[1], J. L. Zhang[1], J. Q. Zhang[1], J. W. Zhang[1], J. Y. Zhang[1], J. Z. Zhang[1], K. Zhang[1], L. Zhang[1], S. H. Zhang[1], X. Y. Zhang[32], Y. Zhang[1], Y. H. Zhang[1], Y. T. Zhang[44], Z. H. Zhang[5], Z. P. Zhang[44], Z. Y. Zhang[49], G. Zhao[1], J. W. Zhao[1], J. Y. Zhao[1], J. Z. Zhao[1], Lei Zhao[44], Ling Zhao[1], M. G. Zhao[29], Q. Zhao[1], Q. W. Zhao[1], S. J. Zhao[51], T. C. Zhao[1], Y. B. Zhao[1], Z. G. Zhao[44], A. Zhemchugov[22,h], B. Zheng[45], J. P. Zheng[1], W. J. Zheng[32], Y. H. Zheng[40], B. Zhong[27], L. Zhou[1], Li Zhou[29], X. Zhou[49], X. K. Zhou[44], X. R. Zhou[44], X. Y. Zhou[1], K. Zhu[1], K. J. Zhu[1], S. Zhu[1], X. L. Zhu[38], Y. C. Zhu[44], Y. S. Zhu[1], Z. A. Zhu[1], J. Zhuang[1], B. S. Zou[1], J. H. Zou[1]

(BESIII Collaboration)

[1] *Institute of High Energy Physics, Beijing 100049, People's Republic of China*
[2] *Beihang University, Beijing 100191, People's Republic of China*
[3] *Bochum Ruhr-University, D-44780 Bochum, Germany*
[4] *Carnegie Mellon University, Pittsburgh, Pennsylvania 15213, USA*
[5] *Central China Normal University, Wuhan 430079, People's Republic of China*
[6] *China Center of Advanced Science and Technology, Beijing 100190, People's Republic of China*
[7] *COMSATS Institute of Information Technology, Lahore, Defence Road, Off Raiwind Road, 54000 Lahore, Pakistan*
[8] *G.I. Budker Institute of Nuclear Physics SB RAS (BINP), Novosibirsk 630090, Russia*
[9] *GSI Helmholtzcentre for Heavy Ion Research GmbH, D-64291 Darmstadt, Germany*
[10] *Guangxi Normal University, Guilin 541004, People's Republic of China*
[11] *GuangXi University, Nanning 530004, People's Republic of China*
[12] *Hangzhou Normal University, Hangzhou 310036, People's Republic of China*
[13] *Helmholtz Institute Mainz, Johann-Joachim-Becher-Weg 45, D-55099 Mainz, Germany*
[14] *Henan Normal University, Xinxiang 453007, People's Republic of China*

[15] Henan University of Science and Technology, Luoyang 471003, People's Republic of China
[16] Huangshan College, Huangshan 245000, People's Republic of China
[17] Hunan University, Changsha 410082, People's Republic of China
[18] Indiana University, Bloomington, Indiana 47405, USA
[19] (A)INFN Laboratori Nazionali di Frascati, I-00044, Frascati, Italy; (B)INFN and University of Perugia, I-06100, Perugia, Italy
[20] (A)INFN Sezione di Ferrara, I-44122, Ferrara, Italy; (B)University of Ferrara, I-44122, Ferrara, Italy
[21] Johannes Gutenberg University of Mainz, Johann-Joachim-Becher-Weg 45, D-55099 Mainz, Germany
[22] Joint Institute for Nuclear Research, 141980 Dubna, Moscow region, Russia
[23] Justus Liebig University Giessen, II. Physikalisches Institut, Heinrich-Buff-Ring 16, D-35392 Giessen, Germany
[24] KVI-CART, University of Groningen, NL-9747 AA Groningen, The Netherlands
[25] Lanzhou University, Lanzhou 730000, People's Republic of China
[26] Liaoning University, Shenyang 110036, People's Republic of China
[27] Nanjing Normal University, Nanjing 210023, People's Republic of China
[28] Nanjing University, Nanjing 210093, People's Republic of China
[29] Nankai University, Tianjin 300071, People's Republic of China
[30] Peking University, Beijing 100871, People's Republic of China
[31] Seoul National University, Seoul, 151-747 Korea
[32] Shandong University, Jinan 250100, People's Republic of China
[33] Shanghai Jiao Tong University, Shanghai 200240, People's Republic of China
[34] Shanxi University, Taiyuan 030006, People's Republic of China
[35] Sichuan University, Chengdu 610064, People's Republic of China
[36] Soochow University, Suzhou 215006, People's Republic of China
[37] Sun Yat-Sen University, Guangzhou 510275, People's Republic of China
[38] Tsinghua University, Beijing 100084, People's Republic of China
[39] (A)Istanbul Aydin University, 34295 Sefakoy, Istanbul, Turkey; (B)Dogus University, 34722 Istanbul, Turkey; (C)Uludag University, 16059 Bursa, Turkey
[40] University of Chinese Academy of Sciences, Beijing 100049, People's Republic of China
[41] University of Hawaii, Honolulu, Hawaii 96822, USA
[42] University of Minnesota, Minneapolis, Minnesota 55455, USA
[43] University of Rochester, Rochester, New York 14627, USA
[44] University of Science and Technology of China, Hefei 230026, People's Republic of China
[45] University of South China, Hengyang 421001, People's Republic of China
[46] University of the Punjab, Lahore-54590, Pakistan
[47] (A)University of Turin, I-10125, Turin, Italy; (B)University of Eastern Piedmont, I-15121, Alessandria, Italy; (C)INFN, I-10125, Turin, Italy
[48] Uppsala University, Box 516, SE-75120 Uppsala, Sweden
[49] Wuhan University, Wuhan 430072, People's Republic of China
[50] Zhejiang University, Hangzhou 310027, People's Republic of China
[51] Zhengzhou University, Zhengzhou 450001, People's Republic of China

[a] Also at the Novosibirsk State University, Novosibirsk, 630090, Russia
[b] Also at Ankara University, 06100 Tandogan, Ankara, Turkey
[c] Also at the Moscow Institute of Physics and Technology, Moscow 141700, Russia and at the Functional Electronics Laboratory, Tomsk State University, Tomsk, 634050, Russia
[d] Currently at Istanbul Arel University, 34295 Istanbul, Turkey
[e] Also at University of Texas at Dallas, Richardson, Texas 75083, USA
[f] Also at the PNPI, Gatchina 188300, Russia
[g] Also at Bogazici University, 34342 Istanbul, Turkey
[h] Also at the Moscow Institute of Physics and Technology, Moscow 141700, Russia

(BESIII Collaboration)

We present the first upper-limit measurement of the branching fractions of the isospin-violating transitions $\chi_{c0,2} \to \pi^0\eta_c$. The measurements are performed using 106×10^6 $\psi(3686)$ events accumulated with the BESIII detector at the BEPCII e^+e^- collider at a center-of-mass energy corresponding to the $\psi(3686)$ mass. We obtained upper limits on the branching fractions at a 90% confidence level of $B(\chi_{c0} \to \pi^0\eta_c) < 1.6 \times 10^{-3}$ and $B(\chi_{c2} \to \pi^0\eta_c) < 3.2 \times 10^{-3}$.

PACS numbers: 13.25.Gv, 13.20.Gd.

I. INTRODUCTION

Isospin is known to be a good symmetry in the hadronic decays of charmonium states. The decay rates of isospin-symmetry breaking modes are in gen-

eral found to be very small. For example, the branching fraction (B) of the measured isospin-violating transition $\psi(3686) \to \pi^0 J/\psi$ was found to be only $(1.26 \pm 0.02(stat.) \pm 0.03(syst.)) \times 10^{-3}$ [1], whereas for other hadronic transitions such as $\psi(3686) \to \pi^+\pi^- J/\psi$, the branching fraction is $(34.45 \pm 0.30) \times 10^{-2}$ [2] and thus significantly stronger.

Although isospin breaking is found to be very small for the conventional charmonium states, the mysterious $X(3872)$ resonance above the $D\bar{D}$ threshold decays strongly via the transition $X(3872) \to \pi^+\pi^- J/\psi$, where the invariant-mass spectrum of the $\pi^+\pi^-$ pair shows a clear ρ signature [3–6] and, hence, is compatible with an isospin-violating decay. A possible interpretation is that the $X(3872)$ is a molecular state composed of a bound D^{*0}-$\bar{D}^0$ meson pair ([7–10]). Such an explanation is particularly popular, since the mass of the $X(3872)$ is close to the sum of the $\bar{D}^0$ and D^{*0} masses, pointing to a state that could be weakly bound by the exchange of a color-neutral meson, similar to the deuteron. Moreover, in such a scenario, the strong isospin-breaking decay rate of the $X(3872)$ might be explained by the large mass gap between the $D^{*0} - \bar{D}^0$ and the $D^{*+} - D^-$ ($D^+ - D^{*-}$) thresholds [11]. A better understanding of the isospin-breaking mechanism in a complementary and well-established charmonium system below the open-charm threshold could be crucial to shed light on the nature of the $X(3872)$.

On the quark level, the isospin-symmetry is broken due to the electromagnetic interaction and due to differences in the up- and down-quark masses (m_u and m_d). It is, therefore, believed that isospin-breaking decays can be used to access the up- and down-quark mass differences once the electromagnetic effect is either well understood or found to be negligible. An example observable that has been proposed to obtain the quark mass ratio, m_u/m_d, is a measurement of the ratio between the branching fractions of the transitions $\psi(3686) \to \pi^0 J/\psi$ and $\psi(3686) \to \eta J/\psi$. Based on a leading-order QCD multipole expansion [12] and the BESIII measurement of this ratio [1], the up-down quark mass ratio is extracted to be $m_u/m_d = 0.407 \pm 0.006$. This result is smaller than the result, $m_u/m_d = 0.56$, obtained using the Goldstone boson masses from a leading-order chiral-perturbation theory [13]. It is important to understand such a large discrepancy between the values of m_u/m_d obtained on the basis of different theoretical conjectures.

The most promising developments in this field are based upon an effective-field theoretical approach. A non-relativistic effective-field theoretical (NREFT) study by the Jülich and IHEP groups suggests that intermediate (virtual) charmed-meson loops are the dominant source for the isospin breaking in the transition $\psi(3686) \to \pi^0 J/\psi$ [14, 15]. According to the proposed theory, the contribution of charmed-meson loops to the amplitude of the process is enhanced by a factor of $(v/c)^{-1} \sim 2$, where v is the heavy-meson velocity in the loops. Detailed studies of different isospin-violating transitions in charmonium below the $D\bar{D}$ threshold and the effect of virtual charmed-meson loops on the widths of the transitions are described in Ref. [16].

The NREFT calculations described above are based on a first estimate, exploiting diagrams involving the lowest-lying pseudoscalar and vector charmed mesons following heavy-quark symmetry and chiral symmetry. Although these theoretical calculations give qualitative insights in the isospin-breaking mechanisms in charmonium decays, the authors in Ref. [16] state that only with a further developed effective-field theory that includes Goldstone bosons, charmonia, and charmed mesons as the degrees of freedom, it would be possible in the future to extract the light-quark masses from quarkonia decays. Currently, for such a theory, quantitative predictions of individual branching fractions of isospin-forbidden decays of charmonium are difficult, because information on the coupling constants $f_{\psi D\bar{D}}$ between different charmonium states and $D\bar{D}$-mesons is limited. The theory requires constraints from experimental data, in particular from measurements of decay rates of other isospin-violating transitions in charmonium [16].

In this paper, we present an experimental study of the isospin-suppressed transition of the charmonium P-wave states $\chi_{c0,2}$ to the ground state η_c via the emission of the π^0. The $\chi_{c0,2}$ states are obtained via electromagnetic transitions, $\psi(3686) \to \gamma\chi_{c0,2}$, whereby the $\psi(3686)$ resonance is directly populated via the e^+e^- annihilation process. The transition $\chi_{c1} \to \pi^0\eta_c$ is not considered in this analysis since it violates conservation of parity and angular momentum. According to Ref. [16], the dimensionless suppression factor for the loops in $\chi_{c0} \to \pi^0\eta_c$ is 0.2. This factor is smaller than in the process $\psi(3686) \to \pi^0 J/\psi$, however, through the interference with the tree-level amplitude, meson loops may give a significant contribution and cannot be neglected.

II. THE BESIII EXPERIMENT AND DATA SET

The analysis is based on the $\psi(3686)$ data sample accumulated by the BESIII detector in 2009. The total number of $\psi(3686)$ events is $(106.41 \pm 0.86) \times 10^6$ [17], corresponding to an integrated luminosity of 156.4 pb^{-1}. In addition, 42.6 pb^{-1} data collected at a center-of-mass energy of 3.65 GeV, are used to estimate the background from non-resonant processes.

The BEijing Spectrometer III (BESIII), described in detail in Ref. [18], is a detector for τ-charm studies running at the Beijing Electron-Positron Collider (BEPCII). BEPCII is a double-ring e^+e^- collider with a designed peak luminosity of 10^{33} cm^{-2}s^{-1} at a beam current of 0.93 A. The cylindrical core of the BESIII detector consists of a main drift chamber (MDC), a plastic scintillator time-of-flight system (TOF), and an electromagnetic calorimeter (EMC), which are enclosed in a superconducting solenoidal magnet providing a 1 T magnetic field. The solenoid is supported by an octagonal flux-

return yoke with resistive-plate chambers forming a muon counter system. The MDC is a small-cell, helium-based (40% He, 60% C_3H_8) sub-detector consisting of 43 layers and providing an average single-hit resolution of 135 μm, and a charged-particle momentum resolution of 0.5% at 1 GeV/c. The EMC sub-detector consists of 6240 CsI(Tl) crystals in a cylindrical structure (barrel) and two end-caps. For 1 GeV photons, the energy resolution is 2.5% (5%) and the position resolution is 6 mm (9 mm) for the barrel (end-caps). The TOF system consists of 5 cm thick scintillators, with 176 detectors of 2.4 m length in two layers in the barrel and 96 fan-shaped detectors in the end-caps. The barrel (end-cap) time resolution of 80 ps (110 ps) provides 2σ K/π separation for momenta up to 1 GeV.

To optimize the event selection, to estimate background contributions, and to evaluate the detection efficiencies, Monte Carlo (MC) simulated samples are obtained exploiting a realistic model of the detector. For this, the GEANT4-based simulation software BOOST [19] is used which includes the geometry and material description of the BESIII spectrometer, and the detector response. A MC sample based on 106 M inclusive $\psi(3686)$ decays is used to study the background. This inclusive sample is generated with KKMC [20] plus EvtGen [21, 22] and the known branching ratios are taken from the Particle Data Group (PDG) [2], while the unknown ratios are generated according to the Lundcharm model [23]. The decay modes $\chi_{c0,2} \to \pi^0\eta_c$ are not present in the inclusive MC simulation. Signal MC samples are generated to determine the detection efficiency and to model the signal shape. In the MC simulations for the processes presented here, the $\psi(3686) \to \gamma\chi_{cJ}$ decay is assumed to be a pure E1 transition, and the polar angle, θ, follows a distribution of the form $1+\alpha\cos^2\theta$, with $\alpha = 1$ and $1/13$ for $J = 0$ and 2, respectively [24, 25]. The $\chi_{c0,2} \to \pi^0\eta_c$ and $\eta_c \to K^0_S K^\pm\pi^\mp$ decays are assumed to be pure phase-space decays.

III. DATA ANALYSIS

For the identification and selection of $\psi(3686) \to \gamma\chi_{c0,2} \to \gamma\pi^0\eta_c$ events, where $\pi^0 \to \gamma\gamma$, $\eta_c \to K^0_S K^\pm\pi^\mp$, the K^0_S is reconstructed in its decay mode to $\pi^+\pi^-$, resulting in the final state $3\gamma 3\pi K$, where K and π are charged.

A. Event selection

Charged tracks are reconstructed from the MDC hits. For each charged-particle track, its polar angle must satisfy $|\cos\theta| < 0.93$. A good charged-particle track (excluding those coming from a K^0_S) is required to be within 1 cm of the e^+e^- annihilation interaction point (IP), transverse to the beam line and within 10 cm of the IP along the beam axis. Charged-particle identification (PID) is based on combining the energy loss, dE/dx, in the MDC and TOF information to construct PID chi-squared values $\chi^2_{PID}(i)$, that are calculated for each charged-particle track for each particle hypothesis i (pion, kaon).

Photons are reconstructed from isolated showers in the EMC. The showers in the angular range between the barrel ($|\cos\theta| < 0.8$) and end-caps ($0.86 < |\cos\theta| < 0.92$) are poorly reconstructed and excluded from the analysis. Good photon candidates must have a minimum energy of 25 (50) MeV in the barrel (end-cap) regions. EMC timing requirements are used to further suppress noise and energy depositions unrelated to the event.

Events with four charged-particle tracks with a net charge of zero and at least three good photon candidates are retained for further analysis.

K^0_S candidates are reconstructed from secondary vertex fits to all the charged-track pairs in an event (with a pion-mass assumption). Candidates with an invariant mass within 10 MeV/c^2 of the K^0_S nominal mass are considered and the combination with the smallest chi-squared of the vertex fit is chosen. The event is kept for further analysis if the secondary vertex is at least 0.5 cm away from the IP. The reconstructed four-momenta of the π^+ and π^-, corresponding to the K^0_S decay, are used as input for the subsequent kinematic fit. To suppress the $K^0_S K^0_S$ background, the remaining charged-particle tracks are required to not form a good K^0_S candidate. The π^0 candidates are reconstructed from pairs of photons with the invariant mass $M_{\gamma\gamma}$ in the range $0.11 < M_{\gamma\gamma}/(\mathrm{GeV}/c^2) < 0.16$, with the $M_{\gamma\gamma}$ resolution of about 5 MeV/c^2.

The $3\gamma 3\pi K$ candidates are then subjected to a four-constraint (4C) kinematic fit, with the constraints provided by four-momentum conservation. The discrimination of charge-conjugate channels ($K^0_S K^+\pi^-$ or $K^0_S K^-\pi^+$) and the selection of the best photon candidate of the $\psi(3686) \to \gamma\chi_{c0,2}$ transition among multiple candidates are achieved by taking the event with the minimum $\chi^2 = \chi^2_{4C} + \chi^2_{PID}(K) + \chi^2_{PID}(\pi)$, where χ^2_{4C} is the chi-squared of the 4C kinematic fit. The π^0 is reconstructed from the two-photon combination with an invariant mass closest to that of a neutral pion. Events with $\chi^2_{4C} < 50$ and with an invariant mass of the reconstructed η_c, $M_{K^0_S K^\pm\pi^\mp}$, in the range $2.70 < M_{K^0_S K^\pm\pi^\mp}/(\mathrm{GeV}/c^2) < 3.30$ are accepted for further analysis. The maximum value of χ^2_{4C} is determined by optimizing the statistical significance $S/\sqrt{S+B}$ in the η_c signal region, where S (B) is the number of signal (background) events obtained from the signal (inclusive) MC samples. For the estimate of S, the branching fractions of $\chi_{c0,2} \to \pi^0\eta_c$ are assumed to be 10^{-3} in analogy with the isospin-violating process $\psi(3686) \to \pi^0 J/\psi$ [1]. The signal region is defined as $2.90 < M_{K^0_S K^\pm\pi^\mp}/(\mathrm{GeV}/c^2) < 3.05$. The χ_{c0} and χ_{c2} signal regions are defined for transition-photon candidates with energies in the $\gamma\pi^0 K^0_S K^\pm\pi^\mp$ center-of-mass system, E_γ, in the ranges of $0.24 < E_\gamma/(\mathrm{GeV}) < 0.28$ and $0.10 < E_\gamma/(\mathrm{GeV}) < 0.15$, respectively.

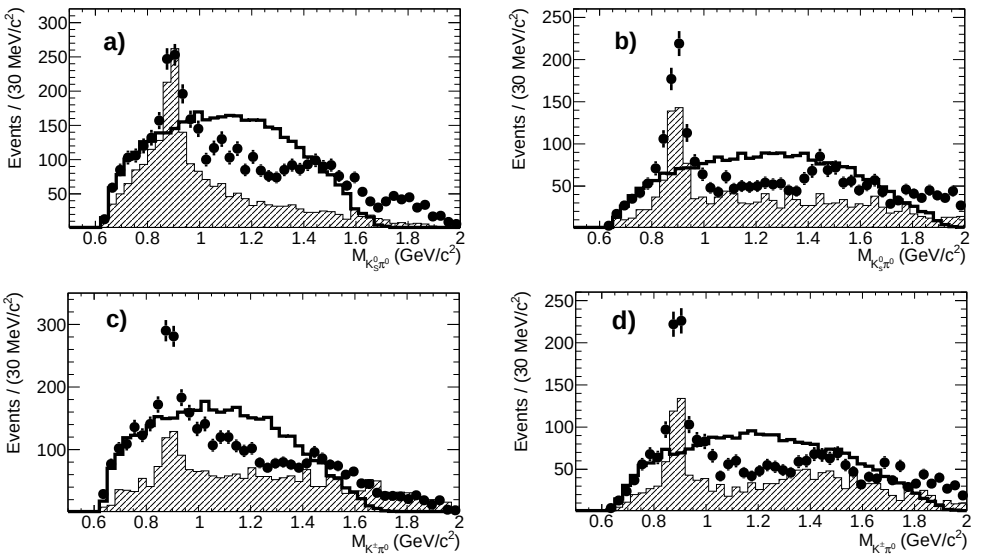

FIG. 1. Invariant-mass distributions of $K^0_S\pi^0$ candidates (a and b) and $K^\pm\pi^0$ candidates (c and d) for χ_{c0} (a and c) and χ_{c2} (b and d) mass regions, respectively. Dots represent data, filled histograms represent inclusive MC results, open histograms show results of signal MC simulations based on a phase-space distribution (arbitrarily scaled).

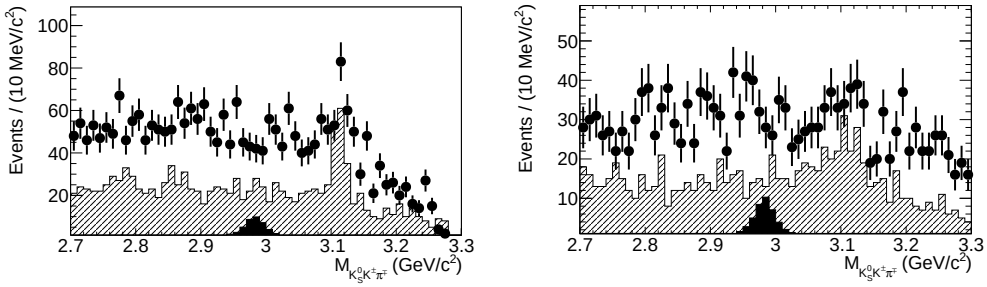

FIG. 2. Invariant-mass distributions of $K^0_SK^\pm\pi^\mp$. Left: $\chi_{c0}\to\pi^0\eta_c$, right: $\chi_{c2}\to\pi^0\eta_c$; $\eta_c\to K^0_SK^\pm\pi^\mp$. Dots represent data, filled histograms represent the inclusive (light) and arbitrarily-scaled signal (dark) MC results. The peak around 3.12 GeV/c^2 is due to the $\psi(3686)\to\pi^0\pi^0J/\psi$ background channel.

FIG. 1 shows the invariant-mass distributions of $K^0_S\pi^0$ candidates (a, b) and $K^\pm\pi^0$ candidates (c, d) with $\pi^0K^0_SK^\pm\pi^\mp$ masses within the χ_{c0} (a, c) and the χ_{c2} (b, d) mass regions. The most prominent peak (with the highest intensity and narrowest width) stems from decays involving a $K^*(892)$. Those are evidently background processes, because the channel of interest, $\chi_{c0,2}\to\pi^0\eta_c$ with $\eta_c\to K^0_SK^\pm\pi^\mp$, cannot involve $K^*(892)^{0(\pm)}\to K^{0(\pm)}\pi^0$ decays, since the latter does not involve a π^0. The regions $0.84 < M_{K^{0(\pm)}_S\pi^0}/(\mathrm{GeV}/c^2) < 0.95$ are excluded in the further analysis to suppress the background from $K^*(892)^0$ and $K^*(892)^\pm$ decays. This condition is optimized to obtain the best statistical significance of the signal.

FIG. 2 shows the invariant-mass distributions of $K^0_SK\pi$ for candidate events with $K^0_SK^\pm\pi^\mp$ masses corresponding to $\chi_{c0,2}\to\pi^0\eta_c$ transitions. The data show no visible peak in the η_c signal region. In the present analysis, upper limits at the 90% confidence level (CL) for the transitions $\chi_{c0,2}\to\pi^0\eta_c$ are determined. Inclusive MC results do not reproduce the number of events found in the data, but reproduce the shape of the invariant-mass distributions of $K^0_SK\pi$ quite well. The discrepancies between data and inclusive MC are primarily due to inaccuracies of branching fractions in the generator and due to mismatches in their corresponding decay dynamics. We note, however, that the inclusive MC data have solely been used to identify background sources and to optimize selection criteria. The selection criteria were optimized by assuming a branching fraction of 10^{-3} for the $\chi_{cJ}\to\pi^0\eta_c$ channels in combination with background taken from the inclusive MC sample. We varied the signal-to-background ratio by a factor of two, adjusted our selection criteria accordingly, and found negligible effect on the precision of our final result.

Efficiencies are calculated using the signal MC simulation samples and are found to be 5.8% and 8.6% for the χ_{c0} and χ_{c2} channels, respectively.

B. Background studies

Background events from $\psi(3686)$ decays are studied with the inclusive MC sample. These studies showed that the channel $\psi(3686) \to \pi^0\pi^0 J/\psi$, $J/\psi \to K^0_S K^\pm\pi^\mp$ results in a peak around 3.12 GeV/c^2 in the $K^0_S K\pi$ invariant-mass spectrum as can be observed from Fig. 2. In this type of transition, one of the photons originating from π^0 decays may escape, which causes a smaller total energy for the event. The kinematic fit increases the energy of the charged-particle tracks, which results in a shift in the invariant mass from 3.10 GeV/c^2 to 3.12 GeV/c^2. This decay channel is taken into account in the final fit to the invariant-mass spectrum of $K^0_S K\pi$ as described below.

The major background contribution stems from the channels $\psi(3686) \to \gamma\chi_{cJ}$, $\chi_{cJ} \to \pi^0 K^0_S K^\pm\pi^\mp$. These channels have final states that are kinematically identical to the signal of interest and, therefore, cannot be removed easily. Partly, this type of background has been suppressed by vetoing $K^*(892)^0$ signals via a cut on the $K^{0,\pm}_S\pi^0$ mass since the background decay, $\chi_{c0,2} \to \pi^0 K^0_S K^\pm\pi^\mp$, contains intermediate $K^*(892)$ resonances, as discussed earlier. We note that the remaining contribution of this type does not result in a peaking background in the signal region.

The background contribution from $e^+e^- \to f\bar{f}$ processes, where $f = e, \mu, d, u, s$, is studied using the continuum data taken at $\sqrt{s} = 3.65$ GeV, and it is found to be negligible. Using the exclusive MC simulations and taking the corresponding branching fractions from the PDG [2], the contribution of $\chi_{cJ} \to \pi^0 K^0_S K^\pm\pi^\mp$ and $\psi(3686) \to \pi^0\pi^0 J/\psi$ channels in the region $2.70 < M_{K^0_S K\pi}/(\mathrm{GeV}/c^2) < 3.30$ is found to be 2260±340 and 1668±260 events for the χ_{c0} and χ_{c2} selection criteria, respectively, where the errors are mainly due to the uncertainties in the branching fractions. The total number of data events in the same region is 2477±50 and 1527±39, respectively. These are compatible within the uncertainties. No significant peaks are observed in the signal region.

C. Upper limits for the number of signal events

To extract the number of η_c events, an unbinned maximum likelihood fit is applied to the candidate events with $K^0_S K^\pm\pi^\mp$ invariant-mass distributions in the region $2.70 < M_{K^0_S K\pi}/(\mathrm{GeV}/c^2) < 3.30$. The η_c signal is described by a Voigtian function, which is a Breit-Wigner function convoluted with the detector resolution. Parameters of the Breit-Wigner function are taken from the PDG [2], and the detector resolution is obtained from a fit to the signal MC set. These parameters are fixed while fitting the data. From the background studies, no peaking background is expected in the signal region. The smooth background is described by a 3^{rd}-order Chebyshev polynomial. A Voigtian function and a Landau plus Gaussian function are used to describe the structure around 3.12 GeV/c^2 for the χ_{c0} and χ_{c2} mass regions, respectively. The line-shape parameters of the structure around 3.12 GeV/c^2 (for both Voigtian and Landau + Gaussian functions) are fixed to the values obtained from the exclusive MC sample. The MC sample was obtained by simulating the channel $\psi(3686) \to \pi^0\pi^0 J/\psi$ with the exclusive decay $J/\psi -> K^0_S K\pi$. The total fit results are shown in FIG. 3. Using the maximum likelihood method, the upper limits on the number of signal events, N^{UL}, at the 90% CL are found to be 14.1 and 35.9 events for the χ_{c0} and χ_{c2} mass regions, respectively.

IV. SYSTEMATIC UNCERTAINTIES

Table I summarizes all the systematic uncertainties that are considered in the analysis. Below we discuss in more detail the individual sources and the procedure that is used to estimate the errors.

The tracking efficiency for kaons as a function of transverse momentum has been studied using the process $J/\psi \to K^0_S K^\pm\pi^\mp$, $K^0_S \to \pi^+\pi^-$ and the tracking efficiency for pions (not originating from K^0_S) as a function of transverse momentum has been studied using the process $\psi(3686) \to \pi^+\pi^- J/\psi$. The difference in efficiencies between data and MC simulations is 2% for each K or π track. This value is taken as the uncertainty in the tracking efficiency. The systematic uncertainty due to the K^0_S reconstruction is 4.0%, as reported in Ref. [26]. The uncertainty in the photon reconstruction is taken as 1% per photon as reported in Ref. [27]. In this analysis, there are in total three photons in the final state, which yields a total systematic uncertainty due to the photon reconstruction of 3%.

Some differences are observed for the χ^2_{4C} distributions between data and MC simulations. These differences are mainly due to inconsistencies in the charged-track parameters between data and MC simulations. We apply correction factors for various K (π) track parameters that are obtained from the control data samples $J/\psi \to \phi\pi^+\pi^-$, $\phi \to K^+K^-$. The correction factors are used for smearing the MC simulation output, so that the pull distributions properly describe those of the experimental data. Differences between the detection efficiencies obtained using MC simulations with and without these corrections are taken as an estimate for the corresponding systematic uncertainties. The uncertainties are 1.2% and 0.8% for the χ_{c0} and χ_{c2} selection conditions, respectively.

A phase-space (PHSP) model used for MC generation of $\eta_c \to K^0_S K^\pm\pi^\mp$ events does not include possible intermediate resonances between the final-state particles, for example, $K^*_2(1430)^{0,\pm}$. These resonances are observed in the test sample $\psi(3686) \to \gamma\eta_c, \eta_c \to K^0_S K^\pm\pi^\mp$. To account for K^* resonances, additional MC samples of $\psi(3686) \to \gamma\chi_{c0,2}, \chi_{c0,2} \to \pi^0\eta_c, \eta_c \to K^*_2(1430)K, K^*_2(1430) \to K\pi$ are generated and the re-

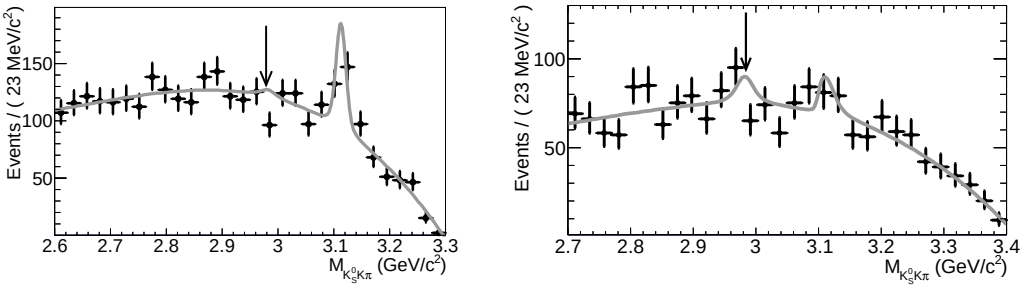

FIG. 3. Fit to the invariant-mass distributions of $K^0_S K^\pm\pi^\mp$. Left: $\chi_{c0} \to \pi^0\eta_c$, right: $\chi_{c2} \to \pi^0\eta_c$; $\eta_c \to K^0_S K^\pm\pi^\mp$. Dots represent data, lines represent the fit. Arrows indicate the peaks of interest.

construction efficiencies are calculated. The difference between efficiencies obtained with two different generator models is taken as a systematic uncertainty. For the $\chi_{c0} \to \pi^0\eta_c$ and $\chi_{c2} \to \pi^0\eta_c$ decays, the corresponding systematic uncertainties are 1.6% and 2.7%, respectively.

The selection of exactly four charged-particle tracks before the vertex cuts can introduce an additional systematic uncertainty in the efficiency determination due to the presence of fake tracks from misreconstruction. This uncertainty is estimated using a sample of $\psi(3686) \to \pi^+\pi^- J/\psi$, $J/\psi \to \gamma\eta_c$, $\eta_c \to K^0_S K^\pm\pi^\mp$ decays, where events with at least six charged-particle tracks are accepted. The fraction of events with more than six tracks compared to the number of events with exactly six charged-particle tracks are obtained for the data and for a corresponding signal MC sample, and the difference in the fractions is found to be 1%. This we take as the systematic uncertainty due to the preselection of exactly four charged-particle tracks.

To estimate the systematic uncertainties due to the resolution of the transition photon, a smearing of the energy resolution by 1.5 MeV and a shift of 0.5 MeV are introduced on the MC data. The smearing gives a minimum χ^2 when comparing data and MC line shapes, where the dominant contribution to the data originates from the processes $\psi(3686) \to \gamma\chi_{cJ}$, $\chi_{cJ} \to \pi^0 K^0_S K^\pm\pi^\mp$. The corresponding detection efficiencies of the channels of interest with the standard selection criteria have been calculated. The largest difference between the efficiencies with and without smearing for the $\chi_{c0,2}$ is 0.6%, which we quote as the systematic uncertainty due to the transition-photon resolution.

The systematic uncertainty due to fitting consists of four parts: uncertainties due to the fitting range, the J/ψ-related background shape, the $\chi_{c0,2} \to \pi^0 K^0_S K\pi$ background shape, and the signal shape. The upper limits for the $2.70 < M_{K^0_S K\pi}/(\mathrm{GeV}/c^2) < 3.30$ fitting range with a 3^{rd}-order Chebyshev function and fixed J/ψ parameters are taken as the nominal upper limit, N^{UL}. By varying the fitting ranges ($2.60 < M_{K^0_S K\pi}/(\mathrm{GeV}/c^2) < 3.30$ and $2.70 < M_{K^0_S K\pi}/(\mathrm{GeV}/c^2) < 3.40$ for the χ_{c0} and χ_{c2} mass regions, respectively), we obtained a set of upper limits from which we take the maximum difference as a systematic uncertainty. The uncertainty is found to be 5.8% and 15.0% for the χ_{c0} and χ_{c2} mass regions, respectively. By changing the parameters for the J/ψ background from fixed to free, but using the nominal fitting range and the nominal order of Chebyshev polynomial, the result of the fitting procedure is obtained, and the relative difference with the nominal upper limit is taken as as a systematic error due to the line shape uncertainty of the J/ψ-related background. This error is found to be 7.3% and 6.8% for the χ_{c0} and χ_{c2} selection conditions, respectively. By varying the order of the Chebyshev polynomial from the third to second, we obtained a set of upper limits from which we take the relative difference as systematic uncertainty due to the $\chi_{c0,2} \to \pi^0 K^0_S K\pi$ background line shape. The uncertainty is found to be 0.1% and 5.0% for the χ_{c0} and χ_{c2} selection conditions, respectively. By changing the mean of the Voigtian within 1 MeV/c^2 and the width within 1 MeV, thereby taking conservatively into account the uncertainty in the published mass and width of the η_c [2], sets of upper limits are obtained from which we take the maximum difference with the nominal upper limit as systematic uncertainty due to the signal line shape. This uncertainty is found to be 2.3% and 2.5% for the χ_{c0} and χ_{c2} selection conditions, respectively. The various systematic uncertainties on the fitting range and the line shape for the signal and background are highly correlated due to double counting of possible uncertainty contributions. The total systematic uncertainty on fitting is estimated by adding the individual systematic uncertainties in quadrature. The total fitting uncertainty is 9.6% and 17.4% for the χ_{c0} and χ_{c2} selection conditions, respectively.

The systematic uncertainty of the number of $\psi(3686)$ events is estimated to be 0.8% as reported in [17]. The uncertainty originating from the trigger efficiency is estimated to be 0.15% [28].

All the uncertainties on the branching fractions of the decaying particles of the channels of interest are obtained from the PDG [2] and are taken into account in the systematic errors of our measurements. The corresponding values can be found in Tab. I.

Assuming that all the sources are independent, the to-

tal systematic uncertainties $\delta_{0,2}$ are obtained by adding the individual uncertainties in quadrature.

TABLE I. Summary of all considered systematic uncertainties (%). All uncertainties quoted are estimated to be symmetric.

Source	$\chi_{c0} \to \pi^0\eta_c$	$\chi_{c2} \to \pi^0\eta_c$
Tracking of K, π	4.0	4.0
K^0_S reconstruction	4.0	4.0
Photon reconstruction	3.0	3.0
Kinematic 4C fitting	1.2	0.8
PHSP generator model	1.6	2.7
4 charged-particle tracks	1.0	1.0
E_γ resolution	0.6	0.6
Fitting	9.6	17.4
Number of $\psi(3686)$	0.8	0.8
Trigger	0.2	0.2
B($\psi(3686) \to \gamma\chi_{cJ}$) [2]	2.7	3.4
B($\eta_c \to K^0_S K\pi$) [2]	6.8	6.8
B($K^0_S \to \pi^+\pi^-$) [2]	0.1	0.1
Total $\delta_{0,2}$	13.8	20.2

V. RESULTS AND DISCUSSION

The upper limits on the branching fractions of the $\chi_{cJ} \to \pi^0\eta_c$ ($J = 0, 2$) transitions are calculated using:

$$B(\chi_{cJ} \to \pi^0\eta_c) < \frac{N_J^{UL}}{N_\psi \varepsilon_J B(\psi(3686) \to \gamma\chi_{cJ}) B_{int}(1-\delta_J)},$$

where N_J^{UL} are the upper limits on the number of signal events, δ_J is the total systematic uncertainty for the channel with $J = 0, 2$, ε_J is the detection efficiency, $B_{int} = B(\eta_c \to K^0_S K^\pm\pi^\mp) \cdot B(K^0_S \to \pi^+\pi^-) \cdot B(\pi^0 \to \gamma\gamma) = (1.7 \pm 0.3) \cdot 10^{-2}$ [2], and N_ψ is the number of $\psi(3686)$ events [17]. Table II summarizes the final results of the analysis.

TABLE II. Summary of the final results for the χ_{cJ} (J = 0,2) decays.

	$\chi_{c0} \to \pi^0\eta_c$	$\chi_{c2} \to \pi^0\eta_c$
N_J^{UL}	14.1	35.9
ε_J	5.8%	8.6%
δ_J	13.8%	20.2%
$B(\chi_{cJ} \to \pi^0\eta_c)(10^{-3})$	< 1.6	< 3.2

In this work, we presented an analysis with the aim to search for the hadronic isospin-violating transitions $\chi_{c0,2} \to \pi^0\eta_c$ using 106×10^6 $\psi(3686)$ events collected by BESIII through $\eta_c \to K^0_S K^\pm\pi^\mp$ decays. No statistically significant signal is observed and upper limits on the branching fractions for the processes $\chi_{c0,2} \to \pi^0\eta_c$ have been obtained. The results are $B(\chi_{c0} \to \pi^0\eta_c) < 1.6 \times 10^{-3}$ and $B(\chi_{c2} \to \pi^0\eta_c) < 3.2 \times 10^{-3}$. These are the first upper limits that have been reported so far. These limits might help to constrain non-relativistic field theories and provide insight in the role of charmed-meson loops to the various transitions in charmonium and charmonium-like states. Further developments in these theories will be necessary to clarify this aspect.

The obtained upper limit on $B(\chi_{c0} \to \pi^0\eta_c)$ does not contradict the theoretical estimate reported by Voloshin [29] of order (few)$\times 10^{-4}$. In this estimate, the branching fraction has been derived from a leading-order QCD expansion and related to the partial width of the decay $\psi(3686) \to h_c\pi^0$ under the assumption that the overlap integrals for the 2S$\to$1P and 1P$\to$1S are of similar value. In addition, Voloshin [29] predicts that the branching fractions of the hadronic decays $\chi_{c0} \to \pi^0\eta_c$ and $\chi_{c1} \to \pi^+\pi^-\eta_c$ are approximately equal. A comparison of our result with that of an upper limit measurement of $B(\chi_{c1} \to \pi^+\pi^-\eta_c < 3.2 \times 10^{-3})$ by BESIII [30] does not contradict such a prediction. We note, however, that an earlier theoretical estimate in the framework of a QCD multipole expansion [31] reported a branching fraction for $\chi_{c1} \to \pi\pi\eta_c$ of (2.22$\pm$1.24)%, which contradicts the earlier BESIII measurement [30] and, under the assumption made by Voloshin [29], our result as well.

The near-future PANDA experiment [32] at the FAIR facility has the potential to find evidence or provide tighter constraints for the isospin-forbidden transitions discussed in this paper by directly populating the $\chi_{c0,2}$ states using an intense antiproton beam on a proton target.

VI. ACKNOWLEDGMENTS

The BESIII collaboration thanks the staff of BEPCII and the IHEP computing center for their strong support. This work is supported in part by National Key Basic Research Program of China under Contract No. 2015CB856700; National Natural Science Foundation of China (NSFC) under Contracts Nos. 11125525, 11235011, 11322544, 11335008, 11425524; the Chinese Academy of Sciences (CAS) Large-Scale Scientific Facility Program; Joint Large-Scale Scientific Facility Funds of the NSFC and CAS under Contracts Nos. 11179007, U1232201, U1332201; CAS under Contracts Nos. KJCX2-YW-N29, KJCX2-YW-N45; 100 Talents Program of CAS; INPAC and Shanghai Key Laboratory for Particle Physics and Cosmology; German Research Foundation DFG under Contract No. Collaborative Research Center CRC-1044; Istituto Nazionale di Fisica Nucleare, Italy; Ministry of Development of Turkey under Contract No. DPT2006K-120470; Russian Foundation for Basic Research under Contract No. 14-

07-91152; U. S. Department of Energy under Contracts Nos. DE-FG02-04ER41291, DE-FG02-05ER41374, DE-FG02-94ER40823, DESC0010118; U.S. National Science Foundation; University of Groningen (RuG) and the Helmholtzzentrum fuer Schwerionenforschung GmbH (GSI), Darmstadt; WCU Program of National Research Foundation of Korea under Contract No. R32-2008-000-10155-0

[1] M. Ablikim *et al.* (BESIII Collaboration), Phys. Rev. D **86**, 092008 (2012).
[2] K. A. Olive *et al.* (Particle Data Group), Chin. Phys. C **38**, 090001 (2014).
[3] S.-K. Choi *et al.* (Belle Collaboration), Phys. Rev. Lett. **91**, 262001 (2003).
[4] S.-K. Choi *et al.* (Belle Collaboration), Phys. Rev. D **84**, 052004 (2004).
[5] A. Abulencia *et al.* (CDF Collaboration), Phys. Rev. Lett. **96**, 102002 (2006).
[6] S. Chatrchyan *et al.* (CMS Collaboration), JHEP **04**, 154 (2013).
[7] F. E. Close and P. R. Page, Phys. Lett. B **578**, 119 (2004).
[8] N. A. Törnqvist, Phys. Lett. B **590**, 209 (2004).
[9] M. Voloshin, Phys. Lett. B **579**, 316 (2004).
[10] E. S. Swanson, Phys. Lett. B **598**, 197 (2004).
[11] N. Li and S.-L. Zhu, Phys. Rev. D **86**, 074022 (2012).
[12] M. A. Shifman and B. L. Ioffe, Phys. Lett. B **95**, 99 (1980).
[13] S. Weinberg, Trans. New York Acad. Sci. **38**, 185 (1977).
[14] F.-K. Guo, C. Hanhart, and U.-G. Meißner, Phys. Rev. Lett. **103**, 082003 (2009).
[15] F.-K. Guo, C. Hanhart, and U.-G. Meißner, Phys. Rev. Lett. **104**, 109901(E) (2010).
[16] F.-K. Guo, C. Hanhart, G. Li, U.-G. Meißner, and Q. Zhao, Phys. Rev. D **82**, 034025 (2010).
[17] M. Ablikim *et al.* (BESIII Collaboration), Chin. Phys. C **37** (2013).
[18] M. Ablikim *et al.* (BESIII Collaboration), Nuclear Instruments and Methods in Physics Research A **614**, 345 (2010).
[19] Z. Y. Deng *et al.*, Chin. Phys. C **30** (2006).
[20] S. Jadach, B. F. L. Ward, and Z. Was, Computer Physics Communications **130**, 260 (2000).
[21] D. J. Lange, Nucl. Instrum. Meth. A **462**, 152 (2001).
[22] R.-G. Ping, Chin. Phys. C **32**, 599 (2008).
[23] J. C. Chen, G. S. Huang, X. R. Qi, D. H. Zhang, and Y. S. Zhu, Phys. Rev. D **62**, 034003 (2000).
[24] G. Karl, S. Meshkov, and J. L. Rosner, Phys. Rev. D **13**, 1203 (1976).
[25] P. K. Kabir and A. J. G. Hey, Phys. Rev. D **13**, 3161 (1976).
[26] M. Ablikim *et al.* (BESIII Collaboration), Phys. Rev. D **87**, 052005 (2013).
[27] M. Ablikim *et al.* (BESIII Collaboration), Phys. Rev. D **83**, 112005 (2011).
[28] N. Berger *et al.* (BESIII Collaboration), Chin. Phys. C **34**, 1779 (2010).
[29] M. B. Voloshin, Phys. Rev. D **86**, 074033 (2012).
[30] M. Ablikim *et al.* (BESIII Collaboration), Phys. Rev. D **87**, 012002 (2013).
[31] Q. Lu and Y.-P. Kuang, Phys. Rev. D **75**, 054019 (2007).
[32] W. Erni *et al.* (PANDA Collaboration), arXiv:0903.3905 [hep-ex].